Original article

Synthesis, anticancer activities and molecular modeling studies of novel indole retinoid derivatives

A. Selen Gurkan-Alp [a,*], Mine Mumcuoglu [b], Cenk A. Andac [c], Emre Dayanc [b], Rengul Cetin-Atalay [b], Erdem Buyukbingol [a]

[a] Department of Pharmaceutical Chemistry, Faculty of Pharmacy, Ankara University, Tandogan, Ankara 06100 Turkey
[b] Department of Molecular Biology and Genetics, Faculty of Science, Bilkent University, Bilkent, Ankara 06100 Turkey
[c] Department of Pharmacology, School of Medicine, Dicle University, Diyarbakir 21280, Turkey

A R T I C L E   I N F O

A B S T R A C T

In this study, novel (E)-3-(5-substituted-1H-indol-3-yl)-1-(5,5,8,8-tetramethyl-5,6,7,8-tetrahydronaphthalen-2-yl)prop-2-en-1-one (5(a–e)) derivatives were synthesized and their anticancer effects were determined in vitro. Novel indole retinoid compounds except 5e have anti-proliferative capacity in liver, breast and colon cancer cell lines. This anti-proliferative effect was further analyzed in breast cancer cell line panel by using the most potent compound 5a. It was determined that 5a can inhibit proliferation at very low IC_{50} concentrations in all of the breast cancer cell lines. Here, we present some evidence on apoptotic termination of cancer cell proliferation which may be primarily driven by the inhibition of RXRα and, to a lesser extent, RXRγ.

© 2012 Elsevier Masson SAS. All rights reserved.

1. Introduction

The indole ring has been deemed as an important moiety found in many pharmacologically active compounds possessing certain biological activities in which some studies have been attributed to its anticancer effectiveness as described in the literature [1–3]. On the other hand, retinoids, natural and synthetic derivatives of vitamin A and its most active metabolite all-trans-retinoic acid have important functions in cell growth, differentiation, modulation of apoptosis and many physiological processes such as vision and embryonic development in vertebrates [4,5]. There are two classes of retinoid nuclear receptors, retinoic acid receptors (RARs) and retinoid X receptors (RXRs), both having three subtypes (α, β, γ) [6]. Retinoid compounds have shown their biological activities via these receptors in which several mechanistic studies have been relied on the magnitude of their influences on these receptors. The properties of retinoids confer a significant therapeutic potential for the treatment of dermatological diseases [7] and cancer, including chemotherapeutic and chemo-preventive applications [8,9]. There is important evidence that these agents have potent growth inhibiting activities on cancer cell lines in vitro and in vivo [4]. In vitro studies and animal models show that retinoids have ability to inhibit carcinogenesis in different tissues [10]. Retinoids have been evaluated as chemo-preventive agents in cancer treatment and prevention. Retinoid compounds have been used efficiently in the treatment of pre-neoplastic diseases such as cervical dysplasia, leukoplakia and xeroderma pigmentosum. Malignant diseases, especially acute promyelocytic leukemia (APL), a subtype of acute myelogenous leukemia (AML) has been successfully treated with retinoids [11]. Other than leukemia, retinoids have anti-proliferative action in solid tumors such as breast, liver, lung, ovarian, prostate and colon cancer [12,13]. Nevertheless, due to the observation of numerous undesirable side effects i.e. teratogenic activity [14,15], liver and bone toxicity [16], hypervitaminosis A syndrome [17], the short and long term applications of retinoids are limited for the treatment of above-mentioned diseases [18]. Synthesized new retinoid derivatives are required that have increased beneficial properties and reduced adverse effects.

In the present study, a series of novel indole retinoid compounds **5**(**a**–**e**) (Scheme 1) consisting of both indole and tetrahydronaphthalene ring system has been synthesized due to the requirements of finding new compounds in cancer treatments. The indole moiety has been reported to exhibit diverse biological activities including anticancer effects [19]. Therefore, indole ring comprise beneficial features of some of the existing anticancer compounds, such as Panobinostat [20,21], Cediranib [22], indole-3-carbinol [23]. On the other hand, natural and/or synthetic retinoids have been known influences to regulate inner cell functions to interfere for the supression of cancer initiation as well as treatment of the certain cancer occurrences [24]. Therefore, we aimed to combine the structural features of tetrahydronaphthalene ring system (retinoid head) and indole moiety with a linker. The antitumoral profiles of the synthesized compounds were investigated.

2. Chemistry

The synthetic procedures for the preparation of the compounds **5**(**a**–**e**) are shown in Scheme 1. Commercially available 2,5-dimethyl-2,5-hexandiole and appropriate 5-*substituted* indole derivatives served as starting materials. 2,5-Dichloro-2,5-dimethyl hexane (**1**), was prepared in 55% yield by passing dry hydrogen chloride gas over 2,5-dimethyl-2,5-hexandiole [18,25]. Benzene was alkylated by compound **1** in dichloromethane catalyzed with aluminum chloride to produce 1,1,4,4-tetramethyl-1,2,3,4-tetrahydronaphthalene (**2**), in 48% yield [26]. Then, 1-(5,5,8,8-tetramethyl-5,6,7,8-tetrahydronaphthalen-2-yl)ethanone (**3**) was obtained by acetylation of intermediate **2** with acetyl chloride using AlCl₃ as a catalyst [26,27]. On the other hand, the corresponding aldehydes **4**(**a**–**e**) were obtained by treating indole derivatives bearing substituent at position 5 with dimethylformamide, using phosphorus oxychloride as a catalyst according to literature method [28–31]. The final compounds (E)-3-(5-*substituted*-1H-indol-3-yl)-1-(5,5,8,8-tetramethyl-5,6,7,8-tetrahydronaphthalen-2-yl)prop-2-en-1-one derivatives **5**(**a**–**e**) were prepared by the condensation of compound **3** with appropriate indole-3-carbaldehyde **4**(**a**–**e**) under basic conditions [32]. Details are stated in the Experimental section.

3. Results and discussion

In this study, we aimed to synthesize novel indole retinoid compounds which are expected to have anticancer properties. To achieve this, five novel indole retinoid derivatives with the substituents at 5th position of the indole ring expected to possess anticancer activity were designed and synthesized. The substitution pattern on the indole ring is thought to have a deterministic factor over the biological effectiveness of the compounds. Due to the distinctive properties of the substituents regarding to their physicochemical behaviors, it might be the way of finding of what relativeness are able to attract activity-inquires leading to exert the desired biological activities. In spite of the fact that the absence of any kind of substitution (hydrogen only) gave the most effectiveness, both electron-donating and electron-withdrawal substitutions had lesser effects in terms of possessing the activity. Actually, this could be a very interesting point of view to support the indole ring system to avoid substituent-inclusion with the enormously activating and/or deactivating substituents rather than using no substitution (like hydrogen only) or with substituents having mild activating/deactivating properties for the future progressions. Thus, more efficiently activating/deactivating substituents could be unfavorable for the biological activity studied.

(E)-3-(5-*Substituted*-1H-indol-3-yl)-1-(5,5,8,8-tetramethyl-5,6,7,8-tetrahydronaphthalen-2-yl)prop-2-en-1-one derivatives **5**(**a**–**e**) were synthesized in four steps (Scheme 1). Synthesized compounds were purified by column chromatography using appropriate solvent systems. Expected chemical structures of the compounds have been deduced by mass, NMR spectral findings and elemental analyses
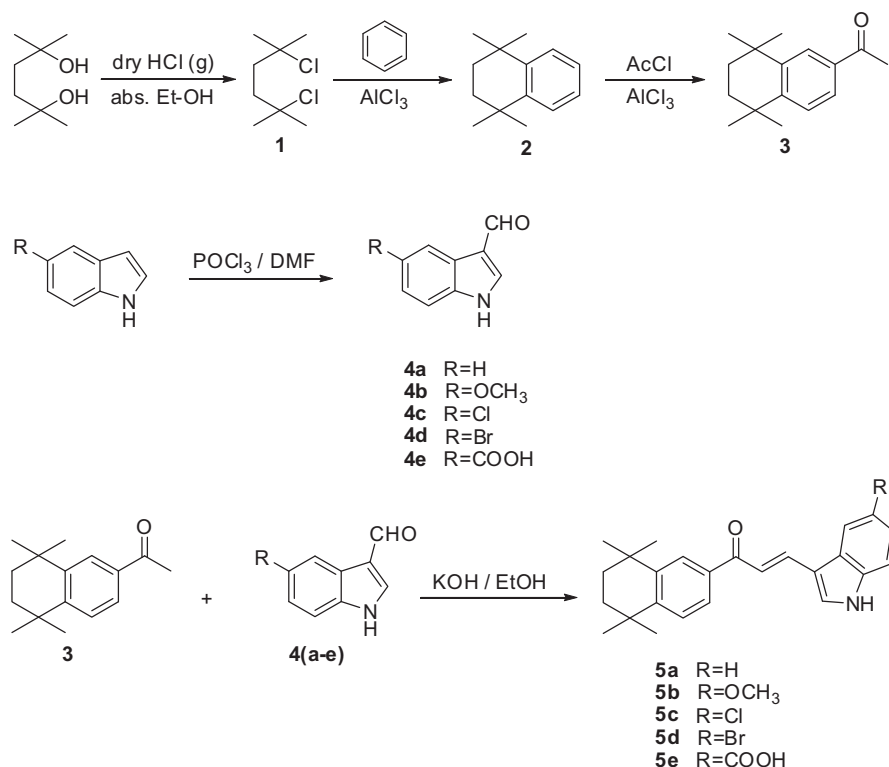
Scheme 1. Synthesis of novel indole retinoid compounds **5**(**a**–**e**).

Table 1

Anti-proliferative capacity of novel indole retinoid derivatives (**5**(**a**–**e**)) evaluated by SRB assay in different types of cancer cell lines. IC_{50} values show μM levels of retinoid concentrations.

Compound	IC_{50} values		
	Huh-7	T47D	HCT116
5a	<0.01	0.10	0.02
5b	15.50	11.37	13.88
5c	15.36	13.14	10.69
5d	13.97	11.54	10.82
5e	no inh.	no inh.	no inh.
CPT	0.06	<0.01	<0.01

Table 2

Anti-proliferative capacity of **5a** analyzed in breast cancer cell line panel. IC_{50} levels of the compound were shown in μM levels. CPT was used as a positive control in the experiment.

	CPT	5a
Cama1	0.07	<0.01
T47D	<0.01	1.16
MCF7	<0.01	1.71
BT474	12.75	1.91
MDA-MB-453	<0.01	<0.01
BT20	<0.01	1.31
SK-BR-3	<0.01	1.29
MDA-MB-361	0.17	0.06
MDA-MB-157	0.02	1.46
MDA-MB-231	<0.01	1.83
ZR-75-1	<0.01	3.88
MCF-12A	<0.01	3.92

indicated in the Experimental section. All spectral data were in accordance with assumed structures. The *trans* conformation of these derivatives were confirmed by a reference $^3J_{HH}$ value of 16 Hz obtained for the HC=CH group of (*E*)-3-(6-fluoro-1*H*-indol-3-yl)acrylic acid [33].

In order to analyze anti-cancer properties of the indole retinoid derivatives, we performed cytotoxicity assay with these derivatives on different types of cancer cell lines. For cytotoxicity studies, we performed sulforhodamine B (SRB) assay [34] determining the IC_{50} values. In this initial screening liver Huh7, breast T47D and colon HCT116, cancer cell lines were treated with these compounds and subjected to SRB assay (Table 1).

SRB assay showed that all of the compounds except compound **5e**, were effective in all three of the cancer cell lines. The compound **5a** had the lowest IC_{50} concentration (nanomolar level) similar to Camptothecin (CPT) among other compounds. In this study, an anti-cancer agent, CPT was included in to the study as an experimental positive control. Therefore, this preliminary result simply implies that the compound **5a** could be a good candidate as an anti-proliferative agent for breast, liver and colon cancer cells.

Retinoids have been known and used for their inhibitory effects on breast cancer in chemoprevention and therapy. Moreover, selective estrogen receptor modulators (SERMs) (tamoxifen, raloxifene etc.) or aromatase inhibitors (AIs) (anastrozole, letrozole etc.) have been used successfully in chemoprevention of estrogen receptor positive (ER-positive) breast cancers [35]. But these drugs cannot prevent the progression of ER-negative breast cancer cases. Herein, the need for new retinoid molecules having the ability of prevention of both ER-positive breast cancers has emerged as one of our concerns. Therefore, we wanted to analyze anti-proliferative effects of compound **5a** on other breast cancer cell lines. For this purpose, we initially analyzed RXRα, RXRγ and ER expression levels by RT-PCR (Fig. 1). The cell lines analyzed had varied ER expression in parallel with RXRγ, but not RXRα. Based on this observation, all

of the 11 breast cancer cell lines and one immortalized normal breast cell line were considered to be screened for the activities of compound **5a** because of their differential ER and RXR expression.

Cells were treated with compound **5a** for three days and then subjected to SRB assay to determine cytotoxicity effect of this compound (Table 2). Cytotoxicity results showed that **5a** can inhibit cancer cell growth at very low drug concentrations in all of the breast cancer cell lines. IC_{50} concentration of **5a** for MCF-12A, which is an immortalized normal epithelial breast cancer cell line, was 3.92 μM. This concentration is four fold higher than IC_{50} concentration of other breast cancer cell lines. This result might provide evidence that if **5a** is utilized as a drug in cancer prevention or treatment in breast cancer, it will be less toxic to normal breast tissue. Breast cancer is a very heterogeneous disease and gene expression profiling analysis revealed presence of different molecular subtypes of breast cancer. These subtypes are luminal A, luminal B, ERBB2-positive, basal-like and normal-like [36]. Every subtype exhibits specific therapeutic response to therapy and prognosis [37]. Breast cancer cell lines used in this study represent all these different subtypes [38]. Compound **5a** effectively blocked proliferation of all these distinct subtypes. Other important aspects of the results were that compound **5a** showed effective anti-proliferative action at very low concentrations even in MDA-MB-231 cell line which is an example of triple-negative breast cancers. Characteristics of triple-negative breast cancer are no expression of estrogen receptor (ER), progesterone receptor (PR) and HER-2 genes. Therefore, they present clinical challenge because they do not respond to endocrine therapy or other available therapies. Furthermore, this subtype of breast cancers shows overall worst or disease free survival [39]. Therefore, compound **5a** could
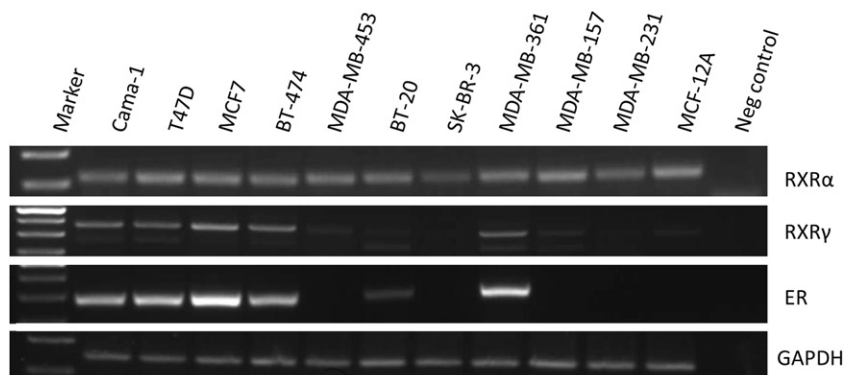

Fig. 1. RXRα, RXRγ and ER expressions were determined in breast cancer cell lines by RT-PCR method.

be a promising drug candidate for the treatment of triple-negative breast cancers.

Retinoids have been known to regulate cell growth, differentiation and apoptosis [40]. Therefore we investigated whether compound **5a** could generate its anti-proliferative effect in breast cancer cells through induction of apoptosis. It was then decided to perform Hoechst staining which is one the apoptosis detection methods for **5a** treated cells. We conducted this assay on T47D and MDA-MB-231 cell lines as representatives of ER-positive and ER-negative groups of breast cancer cells. These cells were treated with **5a** for three days starting from 24 h after seeding. Then treated cells were stained with Hoechst and visualized under florescent microscope for **5a** induced apoptosis. Apoptotic cells were detected after treatment with compound **5a** on both T47D and MDA-MB-231 cell lines compared to DMSO controls (Fig. 2).

To measure the percentage of apoptotic cells, we used flow cytometry analysis. MDA-MB-231 cells were treated with two different concentrations of **5a**, IC_{50} (1.8 µM) and IC_{100} (3.6 µM), and treatment was stopped on day 2 and day 4 for Annexin V and Propidium iodide staining by flow cytometry (Fig. 3). We observed %7.10 and %10.53 of apoptotic cells among the **5a** (1.8 µM) treated cell population on days 2 and 4, respectively. Whereas **5a** (3.6 µM) treated cells were found %6.83 and %15.62 apoptotic on the same days. Therefore we concluded that four days of **5a** treatment at 3.6 µM concentration led to fifty percent increase in apoptotic cell percentage when compared to two days of **5a** treatment.

It has been shown that all-*trans*-retinoic acid and other retinoids can induce apoptosis in breast cancer cell lines [41,42]. This study provided evidences that our novel retinoid compound, **5a**, exerts anti-proliferative effects through induction of apoptosis. Additionally flow cytometry analysis results showed that apoptotic effect of **5a** was gradually increased from day 2 to day 4. This implies that treatment duration of **5a** was an important factor on apoptotic response which was started from day 4. But this proapoptotic property needs further analysis to better understand the precise mechanism of action of compound **5a**.

To gain more insight into the binding mechanism and estimate binding affinity at the molecular level, compound **5a** was initially docked into the binding site of RXR-alpha (RXRα) (PDB ID: 2ZXZ [43]) and RXR-gamma (RXRγ) (PDB ID: 4LBD [44]). Coordinates for
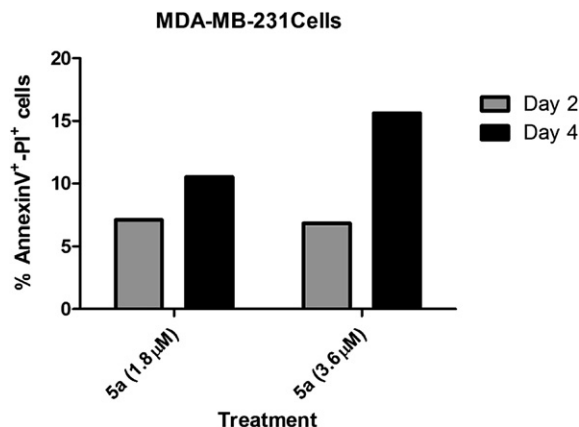

Fig. 3. Flow cytometry analysis. MDA-MB-231 breast cancer cell line cells were seeded, and after 24 h, cells were treated with two different concentrations of **5a** (1.8 µM and 3.6 µM). Measurements were made on two days and four days post-treatment. The rate of apoptosis was determined by Annexin V and Propidium iodide staining, and mean percentage of Annexin V+ and Propidium Iodide+ cells were plotted against treatment modalities. Gray bars represent Day 2, and black bars represent Day 4 of treatment.

the pharmacophore tetramethyltetrahydro naphthalene group in the original PDB files were referenced to select the lowest r.m.s.d. docked coordinates of compound **5a** in the binding site of RXRα and RXRγ. The preference for this binding mode of compound **5a** relies greatly on the fact that the indole group of compound **5a**, which superimposed with the carboxylic acid side of all-*trans*-retinoic acid in another set of docking studies implemented using the crystal structure of all-*trans*-retinoic acid in complex with RXRγ (PDB ID: 2LBD [45]), is more polar than the tetramethyltetrahydro naphthalene group of compound **5a**, which superimposed with the trimethyl-cyclohexen group of all-*trans*-retinoic acid in the binding site of RXRγ [45]. After docking studies, 10 ns of molecular dynamics (MD) computations were applied for docked coordinates of compound **5a** in the binding site of RXRα and RXRγ. Although MD computations equilibrated beyond 4 ns, the MD solution structures of the complex species were sampled and monitored between 9 and 10 ns of trajectories in order to assure stability during sustained equilibration. The MD computations revealed that
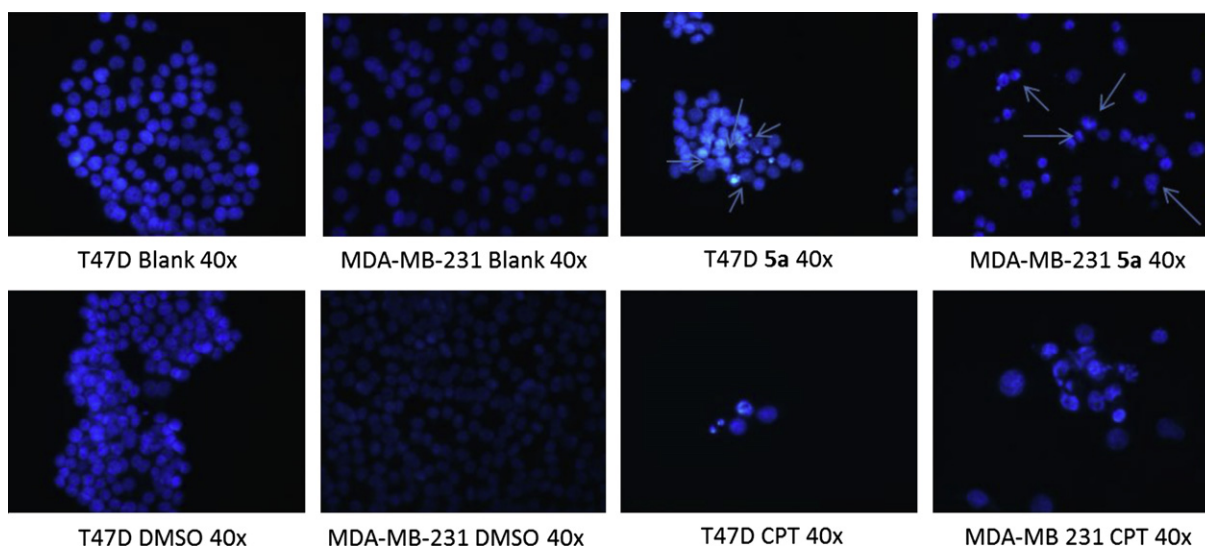

Fig. 2. Hoechst staining. T47D and MDA-MB-231 cells were treated with compound **5a** for three days and stained with Hoechst. Arrows show apoptotic cells. Pictures were taken at 40× objective magnification. Camptothecin (CPT) was used as a positive control in the experiment.
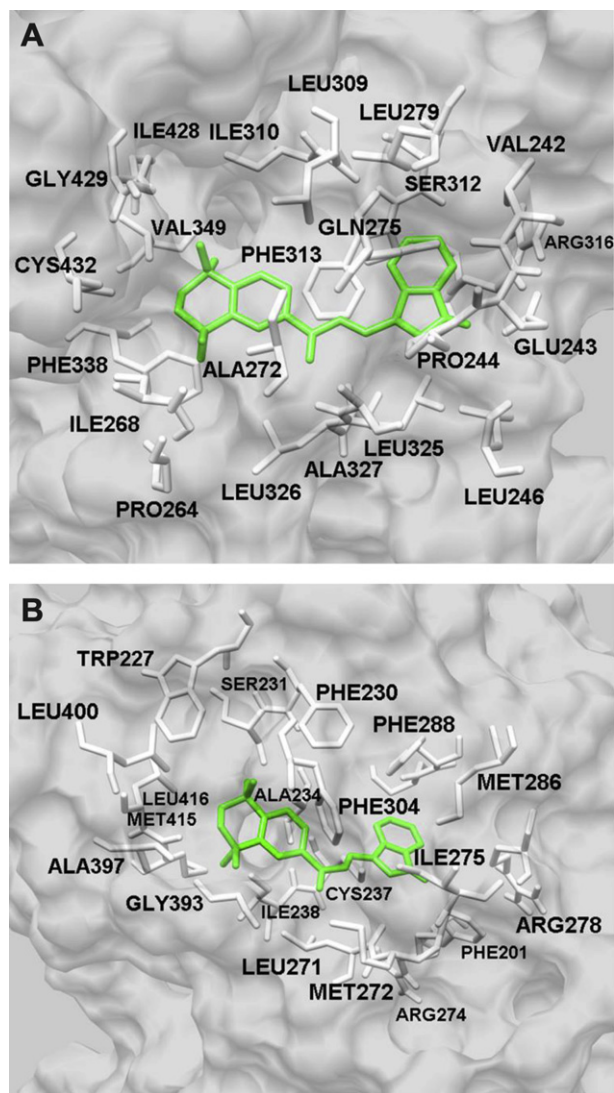
Fig. 4. Compound **5a** (green) confined to the binding site of (A) RXRα and (B) RXRγ at 10 ns of MD computation. Amino acid residues neighboring compound **5a** are annotated in black. (For interpretation of the references to colour in this figure legend, the reader is referred to the web version of this article.)

compound **5a** is mainly confined to the binding sites of RXRα, Fig. 4A, and RXRγ, Fig. 4B.

MM−PBSA binding enthalpy energy terms are listed in Table 3. It was determined that compound **5a** possesses very high binding affinities toward RXRα ($\Delta G° = -20.19$ kcal/mol, $K_D = 1.9 \times 10^{-15}$ kcal/mol) and RXRγ ($\Delta G° = -13.13$ kcal/mol, $K_D = 2.7 \times 10^{-10}$ kcal/mol).

Table 3
MMPBSA binding energies (kcal/mol) and dissociation constants K_D (kcal/mol) for compound **5a**.

	RXRα	RXRγ
ΔE_{el}	-23.53 ± 3.25	-10.45 ± 3.24
ΔE_{VDW}	-56.16 ± 2.70	-51.25 ± 2.74
ΔE_{int}	0.00 ± 0.01	-0.01 ± 0.01
ΔH_{gas}	-79.69 ± 3.69	-61.71 ± 4.19
ΔG_{nonel}	-6.87 ± 0.12	-6.97 ± 0.13
ΔG_{el}	45.69 ± 2.86	37.51 ± 3.07
$\Delta H°$	-40.87 ± 3.85	-31.18 ± 4.74
$T \cdot \Delta S°$	-20.68 ± 10.92	-18.05 ± 7.71
$\Delta G°$	-20.19	-13.13
K_D	1.9×10^{-15}	2.7×10^{-10}

Since RXRα possesses the highest binding affinity, we suggest that the anti-proliferative effect of compound **5a** could be more likely related to this receptor rather than RXRγ.

Definitions of the energy terms in Table 3 are given in Section 5.3.3. K_D was determined according to a generic equation, $\Delta G° = -R \cdot T \ln (1/K_D)$, where $\Delta G°$ is the binding free energy in kcal/mol, T is the temperature at 300 K and R is the ideal gas constant, 1.987 cal/mol K. MM−PBSA computations revealed that a total of non-electrostatic contributions [ΔE_{VDW} (gas) $+ \Delta G_{nonel}$ (solution)] to the enthalpy of binding are favorable for the RXRα · compound **5a** (-63.03 kcal/mol) and RXRγ · compound **5a** (-58.22 kcal/mol) complex systems, strongly suggesting that compound **5a** possesses a hydrophobic nature and thus it prefers to interact with hydrophobic binding sites. However, electrostatic contributions [ΔE_{el} (gas) $+ \Delta G_{el}$ (solution)] to the enthalpy of binding were found to be unfavorable for compound **5a** in complex with RXRα (23.16 kcal/mol) and RXRγ (27.06 kcal/mol), in which case an energy difference of 3.90 kcal/mol disfavoring the RXRγ · compound **5a** complex species suggest that the binding site of RXRα possesses slightly more hydrophobic amino acid residues (VAL242, GLU243, PRO244, LEU246, PRO264, ILE268, ALA272, GLN275, LEU279, LEU309, SER312, PHE313, ARG316, LEU325, LEU326, ALA327, PHE338, VAL349, ILE428, GLY429, CYS432), Fig. 4A, than that of RXRγ (PHE201, TRP227, PHE230, SER231, ALA234, CYS237, ILE238, LEU271, MET272, ARG274, ILE275, ARG278, MET286, PHE288, PHE304, GLY393, ALA397, LEU400, MET415, LEU416), Fig. 4B.

After determination of binding mechanism and affinity of **5a** to RXRα and RXRγ, we checked the expression level of these two receptors in our breast cancer cell lines. RXRα was expressed in all of the breast cancer cell lines. Nevertheless RXRγ expression was absent in SK-BR-3 and MDA-MB-231 cell lines. Since compound **5a** showed high binding affinity pattern toward both RXRα and RXRγ, *in silico*, still there could be an ambiguous explanation of the data obtained from *in vitro* biological assays and molecular dynamics. In this case, there seems to be a conflict between *in vitro* experimental results and molecular dynamics predictions. The molecular dynamics predictions showed high binding affinities for both receptors whereas *in vitro* experimental results indicated the existence of RXRα expression, but not RXRγ. This observation may point out that *in silico* prediction approaches are quite far from the explanation of accurate interaction patterns of *in vivo* ligand−receptor relationships. Molecular dynamics studies obviously provide a road-map for such interactions to assume the consideration of possible mechanisms for the biological phenomena.

More likely, different mechanisms could be attributed if there were being utilized with different cancer cell lines which have an expression of RXRγ. But in our case, RXRα was found to have the main factor, which is responsible in the occurrence of the biological activity. The other receptor involvements were not included in this study due to the main approach has been focused on the RXRα. However, studies for finding out though different mechanisms are under progress.

4. Conclusions

Breast cancer is the second leading cause of cancer death in women in the world. Therefore generation of new agents for the prevention and the treatment of the breast cancer are very critical. Our results have determined that most of our novel indole retinoid compounds have anti-proliferative effects in different cancer cell lines especially in breast cancer cell lines. Compound **5a** showed the lowest IC$_{50}$ level in cytotoxicity assays in our breast cancer cell line panel, which includes ER-positive and ER-negative cell lines. Furthermore, we observed that **5a** was less toxic in MCF-12A, which

is a normal-like breast epithelial cell line. Compound **5a** induced apoptosis was the cause of the anti-proliferative effect. We also performed molecular binding studies to analyze the involvement of retinoic receptors. We predicted that **5a** binds RXRα and RXRγ. These results implied that these novel indole retinoid compounds, particularly **5a**, could be a promising anti-cancer agent candidate in prevention or treatment of different cancers. Nevertheless, further investigation is needed to determine exact mechanisms underlying this effect.

5. Experimental section

5.1. General synthetic

All starting materials and reagents were high-grade commercial products purchased from Aldrich, Merck or Fluka. The structures of all synthesized compounds were assigned on the basis of ^1H NMR and Mass spectral analyses. Analytical thin-layer chromatographies were run on silica gel 60 F_{254} plates (Merck, Germany). Column chromatographies were accomplished on silica gel 60 (40—63 μm particle size) (Merck, Germany). Melting points were determined with an Electrothermal 9100 melting point apparatus (Electrothermal Engineering, Essex, UK) and uncorrected. ^1H NMR (400 MHz) spectra were recorded with a Varian Mercury-400 spectrometer (Varian Inc., Palo Alto, CA, USA), in CDCl$_3$ or DMSO-d_6, δ scale (ppm) from internal standard TMS. Mass spectra were recorded on a Waters ZQ micromass LC—MS spectrometer (Waters Corporation, Milford, MA, USA) by the method of ESI$^+$. Elemental analyses were performed on LECO CHNS-932 instrument (Leco, St Joseph, MI, USA) and satisfactory results ±0.4% of calculated values (C, H, N) were obtained. ^1H NMR, Mass, and elemental analyses were performed at The Central Instrumentation Laboratory of the Pharmacy Faculty of Ankara University, Ankara, Turkey.

5.1.1. General methods for the preparation of the (E)-3-(5-substituted-1H-indol-3-yl)-1-(5,5,8,8-tetramethyl-5,6,7,8-tetrahydronaphthalen-2-yl)prop-2-en-1-one derivatives 5(a—e)

To a solution of 1-(5,5,8,8-tetramethyl-5,6,7,8-tetrahydronaphthalen-2-yl)ethanone (**3**) (2 mmol) and appropriate indole-3-carbaldehyde **4(a—e)** (2 mmol) in 4 ml of ethanol and 2 ml of water was added 2 g of solid KOH. The reaction mixture was refluxed for at least 12 h. The end of the reaction was monitored by TLC. The resulting mixture was cooled in an ice-water bath, and then acidified with 4 ml of concentrated HCl and diluted with 20 ml of water. The precipitate was then collected by filtration and dried [32]. The crude product was purified by column chromatography eluting with n-hexane/ethyl acetate (3:1) solvent system to give **5(a—e)**.

5.1.2. (E)-3-(1H-Indol-3-yl)-1-(5,5,8,8-tetramethyl-5,6,7,8-tetrahydronaphthalen-2-yl)prop-2-en-1-one (5a)

14% Yield, yellow crystalline solid, m.p. 196—198 °C. ESI$^+$-MS (m/z %): 358 (M + H, 100). ^1H NMR δ ppm (CDCl$_3$): 8.62 (br.s, 1H, −NH), 8.09 (d, 1H, J = 15.2 Hz), 8.03 (d, 1H, J_m = 2 Hz), 8.01 (m, 1H), 7.81 (dd, 1H, J_o = 8 Hz, J_m = 1.6 Hz), 7.61 (s, 1H, indole −H(2)), 7.59 (d, 1H, J = 15.6 Hz), 7.45 (m, 2H), 7.31 (m, 2H), 1.73 (s, 4H, −CH$_2$−CH$_2$−), 1.34 (d, 12H, −(CH$_3$)$_2$, −(CH$_3$)$_2$). Elemental analysis, Calcd for C$_{25}$H$_{27}$NO: C 83.99; H 7.61; N 3.92. Found: C 83.71; H 7.47; N 3.86.

5.1.3. (E)-3-(5-Methoxy-1H-indol-3-yl)-1-(5,5,8,8-tetramethyl-5,6,7,8-tetrahydronaphthalen-2-yl) prop-2-en-1-one (5b)

14% Yield, yellow solid, m.p. 138—139 °C. ESI$^+$-MS (m/z %): 388 (M + H, 40). ^1H NMR δ ppm (CDCl$_3$): 8.57 (br.s, 1H, −NH), 8.08 (d, 1H, J = 15.6 Hz), 8.02 (d, 1H, J_m = 1.6 Hz), 7.80 (dd, 1H, J_o = 8.4 Hz, J_m = 2 Hz), 7.59 (d, 1H), 7.51 (d, 1H, J = 15.6 Hz), 7.44 (d, 1H, J_o = 8 Hz), 7.43 (s, 1H, indole −H(2)), 7.33 (d, 1H, J_o = 9.2 Hz), 6.95 (dd, 1H, J_o = 8.8 Hz, J_m = 2 Hz), 3.92 (s, 3H, −OCH$_3$), 1.73 (s, 4H, −CH$_2$−CH$_2$−), 1.34 (d, 12H, −(CH$_3$)$_2$, −(CH$_3$)$_2$). Elemental analysis, Calcd for C$_{26}$H$_{29}$NO$_2$: C 80.59; H 7.54; N 3.61. Found: C 80.34; H 7.79; N 3.33.

5.1.4. (E)- 3-(5-Chloro-1H-indol-3-yl)-1-(5,5,8,8-tetramethyl-5,6,7,8-tetrahydronaphthalen-2-yl)prop-2-en-1-one (5c)

13% Yield, yellow solid, m.p. 195—197 °C. ESI$^+$-MS (m/z %): 392 (M + H, 100), 394 (M + H + 2, 30). ^1H NMR δ ppm (CDCl$_3$): 8.79 (br.s, 1H, −NH), 8.02 (d, 1H, J_m = 2 Hz), 8.01 (d, 1H, J = 16 Hz), 7.96 (d, 1H, J_m = 2 Hz), 7.80 (dd, 1H, J_o = 8.4 Hz, J_m = 2 Hz), 7.61 (d, 1H), 7.52 (d, 1H, J = 15.6 Hz), 7.46 (d, 1H, J_o = 8 Hz), 7.36 (d, 1H, J_o = 8.4 Hz), 7.26 (dd, 1H, J_o = 8.8 Hz, J_m = 2 Hz), 1.73 (s, 4H, −CH$_2$−CH$_2$−), 1.34 (d, 12H, −(CH$_3$)$_2$, −(CH$_3$)$_2$). Elemental analysis, Calcd for C$_{25}$H$_{26}$ClNO−0.55H$_2$O: C 74.72; H 6.79; N 3.48. Found: C 74.88; H 7.16; N 3.08.

5.1.5. (E)-3-(5-Bromo-1H-indol-3-yl)-1-(5,5,8,8-tetramethyl-5,6,7,8-tetrahydronaphthalen-2-yl)prop-2-en-1-one (5d)

18% Yield, a yellow solid, m.p. 199—200 °C. ^1H NMR δ ppm (CDCl$_3$): 8.84 (br.s, 1H, −NH), 8.12 (d, 1H, J_m = 1.6 Hz), 8.02 (d, 1H, J = 1.2 Hz), 8.01 (d, 1H, J = 16 Hz), 7.79 (dd, 1H, J_o = 8.4 Hz, J_m = 2 Hz), 7.58 (d, 1H), 7.51 (d, 1H, J = 16 Hz), 7.46 (d, 1H, J_o = 8.4 Hz), 7.39 (dd, 1H, J_o = 8.8 Hz, J_m = 2 Hz), 7.31 (d, 1H, J_o = 8.4 Hz), 1.73 (s, 4H, −CH$_2$−CH$_2$−), 1.34 (d, 12H, −(CH$_3$)$_2$, −(CH$_3$)$_2$). Elemental analysis, Calcd for C$_{25}$H$_{26}$BrNO: C 68.81; H 6.01; N 3.21. Found: C 68.88; H 5.92; N 3.12.

5.1.6. (E)-3-(3-Oxo-3-(5,5,8,8-tetramethyl-5,6,7,8-tetrahydronaphthalen-2-yl)prop-1-enyl)-1H-indole-5-carboxylic acid (5e)

5% Yield, yellow solid, m.p. 274—275 °C. ESI$^+$-MS (m/z %): 402 (M + H, 100). ESI$^-$-MS (m/z %): 400 (M − H, 80). ^1H NMR δ ppm (DMSO-d_6): 12.69 (br.s, 1H, −NH), 12.19 (s, 1H, −COOH), 8.60 (s, 1H), 8.26 (s, 1H), 8.01 (d, 1H, J = 16 Hz), 7.99 (s, 1H), 7.85 (d, 1H, J_o = 8.4 Hz), 7.78 (d, 1H, J_o = 8.4 Hz), 7.65 (d, 1H, J = 15.2 Hz), 7.55 (m, 2H), 1.70 (s, 4H, −CH$_2$−CH$_2$−), 1.32 (d, 12H, −(CH$_3$)$_2$, −(CH$_3$)$_2$). Elemental analysis, Calcd for C$_{26}$H$_{27}$NO$_3$−0.7H$_2$O: C 75.41; H 6.91; N 3.38. Found: C 75.30 H, 6.79; N 3.22.

5.2. General biological assays

5.2.1. Cell culture

Most of the cell lines were grown in Dulbecco's modified Eagle's medium (DMEM) supplemented with 10% fetal calf serum (FCS) and 50 mg/ml penicillin/streptomycin. CAMA-1 and MDA-MB-157 were grown in DMEM containing 10% FCS, 50 mg/ml penicillin/streptomycin and 1% sodium pyruvate. Glucose rich (4.5 g/l) RPMI medium for ZR-75-1 and McCoy medium for SK-BR-3 were used and supplemented with 10% FCS and 50 mg/ml penicillin/streptomycin. Each cell line was maintained in a humidified incubator at 37 °C supplied with 5% CO$_2$.

5.2.2. Sulforhodamine B (SRB) cytotoxicity assay

Cancer cells (10^4 cells/well) were inoculated into 96 well plates and after 24 h, cells were treated with retinoid compounds. After three days of incubation with retinoids, cells were fixed using 60 μl of ice-cold 10% trichloroacetic acid (TCA) for 60 min at 4 °C. Next 100 μl 0.4% SRB solution was administered and cells were incubated for 10 min at room temperature. To remove unbound dye, cells were washed with 1% acetic acid five times and air dried. 10 mM Tris-Base solution was applied to solubilize SRB dye and absorbance was acquired at 515 nm in micropipette reader. All the experiments were conducted in triplicate and DMSO was used as negative control in corresponding concentrations.

5.2.3. Hoechst staining

Human cancer cells (50.000 cells/well) were seeded into six-well plates and 24 h later retinoid compounds were applied. Hoechst staining was performed after 72 h of incubation with retinoid compounds (IC_{50} concentration). Cells were incubated with 1 μg/ml concentration of Hoechst 33258 (Sigma–Aldrich, 861405) in 1× phosphate buffered saline (PBS) for 5 min at room temperature at dark. Then, the cells were detained with ddH$_2$O for 10 min and mounted onto slides. Apoptotic cells were visualized under a fluorescent microscope (Zeiss, Axiovision Rel 4.6) at 40× objective magnification.

5.2.4. Flow cytometry analysis

Cells were seeded at 5.10^5 cells per well onto 75 mm^2 tissue culture plates and incubated in humidified incubators at 37 °C, with 5% CO$_2$. The next day, cells were treated with two different concentrations of **5a** (1.8 μM and 3.6 μM). On day 2 and day 4, 1.10^6 cells were sampled and stained with FITC Annexin V Apoptosis detection Kit (BD Pharmingen, Cat: 556570) according to the manufacturer's instructions. Control groups include corresponding DMSO concentrations as negative controls and CPT (5 μM) and 1% v/v hydrogen peroxide, as positive controls. Stained cells were kept from light on ice and analyzed immediately using Becton Dickinson FACScalibur Flow Cytometer. Flow cytometry results were analyzed using WinMDI 2.9 software (http://facs.scripps.edu/software.html) for differentially stained percentage of cells over controls and results were plotted and analyzed using GraphPad Prism version 5.00 (GraphPad Software, San Diego California USA).

5.3. Computational studies

5.3.1. System set-up and initial structures

X-ray coordinates for human retinoid X receptor alpha (RXRα) in complex with 4-[2-(1,1,3,3-tetramethyl-2,3-dihydro-1H-inden-5-yl)-1,3-dioxolan-2-yl] benzoic acid and human retinoid X receptor gamma (RXRγ) in complex with 3-fluoro-4-[2-hydroxy-2-(5,5,8,8-tetramethyl-5,6,7,8-tetrahydro-naphtalen-2-yl)-acetylamino] benzoic acid were obtained from Protein Data Bank (PDB ID: 2ZXZ [43] and 4LBD [44], respectively). All ligands and water molecules were initially removed from the X-ray structures. Amino acid residues 245–261 in the X-Ray structure of RXRα are not resolved. In general, the RXRα and RXRγ proteins in the PDB files share 34.35% amino acid sequence identity with very similar three dimensional motifs. Therefore, amino acid backbone (NH–CH–CO–) coordinates for the missing residues of RXRα were obtained from amino acid residues 203–219 in the X-ray structure of RXRγ, whose amino acid residue names were mutated to comply with those of RXRα.

Compound **5a**, shown in Scheme 1 was docked by Auto Dock v4.2 [46] into the binding site of RXRα and RXRγ using a flexible binding site and flexible ligand strategy applied by Auto Dock. Molecular dynamics (MD) and molecular mechanics-Poisson Boltzmann/surface area (MM–PBSA) computations were implemented by AMBER v11 (2010) suite of programs [47] running under 64 bit Scientific Linux at the TR-Grid e-Infrastructure of Turkey. AMBER1999Sbildn [48] and general AMBER force fields (GAFF) [49] were used together to parameterize the RXRα · compound **5a** and RXRγ · compound **5a** complexes for implicit solvent simulations by the LeaP [50] module of AMBER v11.

5.3.2. Molecular dynamics

Temperature equilibration and MD routines were conducted in implicit solvent environment by the parallel pmemd (Particle Mesh Ewald Molecular Dynamics) module of AMBER v10 [47] using a generalized Born solvent model of Onufriev et al. (igb = 5

parameter in pmemd) [51]. The coordinates of the starting structure were initially relaxed to remove bad close contacts over 1000 iterations. The temperature of the relaxed system was then equilibrated at 300 K through 10 ps of MD using 2 fs time steps over 5000 iterations. Langevin dynamics [52] was used to equilibrate the temperature of the system at 300 K by using a collision frequency of 10 ps^{-1} and a velocity limit of 10 temperature units. The final coordinates of the temperature equilibration routine (after 10 ps) were then used to run 10 ns molecular dynamics using 2 fs time steps over 5 million iterations, during which the temperature was kept at 300 K using the same Langevin dynamics parameters as applied before. During the temperature equilibration and MD routines, a non-bonded cutoff distance of 999 Å was applied by the Particle Mesh Ewald method [53] to handle electrostatic interactions in implicit solvent media and SHAKE method [54] was applied to keep the bond lengths of protons attached to heteroatoms constant. Coordinates and energy outputs for the relaxation and the molecular dynamics routines were saved every 5000 iterations.

5.3.3. MM–PBSA computations

MM–PBSA (molecular mechanics–Poisson Boltzmann/surface area) binding energy computations were conducted by the mm–pbsa [55] module of AMBER v11. For the formation of the complex, as generically shown in EQ. (1), MM–PBSA

$$Receptor + Ligand \leftarrow \rightarrow Complex \tag{1}$$

free energy computations were implemented for the complex (RXRα/γ. compound **5a**), receptor (RXRα/γ) and the ligand (compound **5a**). The absolute free energy (G) of the complex systems, their receptors, and the ligand were computed in a classical manner as in EQ. (2), in which T is the temperature of the system at 300 K.

$$G = H - T \cdot S \tag{2}$$

The binding free energies (ΔG) of the complex systems were computed as in EQ. (3) where G_{comp} is the absolute free energy of the complex, G_{rec} is the absolute free

$$\Delta G = G_{comp} - \left[G_{rec} + G_{lig} \right] \tag{3}$$

energy of the receptor, and G_{lig} is the absolute free energy of the ligand. 50 Snapshots were extracted for the coordinates of the solute species (complex, receptor and ligand) at 20 ps time intervals between 9 ns and 10 ns of the trajectories. MM–PBSA energies were computed for each snapshot and averaged out to constitute mean binding free energies (ΔG).

The enthalpy term in EQ. (2) is dissected into subenergy terms as in EQ. (4).

$$H_{tot} = H_{gas} + G_{solv} \tag{4}$$

where H_{gas} is the potential energy of the solute in gas phase which is determined as a sum of van der Waals (E_{VDW}), electrostatic (E_{el}) and internal (E_{int}) energies as in Cornell et al. (1995) force field [54]. G_{solv} is the solvation free energy for transferring the solute from vacuum into solvent and is a sum of electrostatic (G_{el}) and non-electrostatic (hydrophobic) contributions (G_{nonel}) as seen in EQ. (5).

$$G_{solv} = G_{el} + G_{nonel} \tag{5}$$

G_{el} was computed at 0.15 M salt concentration by the pbsa module of AMBER v11. [47] using Poisson Boltzmann equations [55,56]. G_{nonel} was computed by the molsurf module of AMBER v11 [55]. The entropy energy term, S in EQ. (2), was computed for each

solute species by normal-mode analysis [57,58] integrated into the *nmode* module of AMBER v11.

Acknowledgment

References

[1] A. Andreani, M. Granaiola, A. Leoni, A. Locatelli, R. Morigi, M. Rambaldi, V. Garaliene, Synthesis and antitumor activity of 1,5,6-substituted *E*-3-(2-chloro-3-indolylmethylene)-1,3-dihydroindol-2-ones, J. Med. Chem. 45 (2002) 2666–2669.

[2] M. Grugni, M. Cassin, G. Colella, S. De Munari, G. Pardi, P. Pavesi, Indole derivatives with antitumor activity, WO/2006/066923.

[3] A. Andreani, S. Burnelli, M. Granaiola, A. Leoni, A. Locatelli, R. Morigi, M. Rambaldi, L. Varoli, L. Landi, C. Prata, M.V. Berridge, C. Grasso, H.-H. Fiebig, G. Kelter, A.M. Burgere, M.W. Kunkelf, Antitumor activity of bis-indole derivatives, J. Med. Chem. 51 (2008) 4563–4570.

[4] M.B. Sporn, A.B. Roberts, D.S. Goodman (Eds.), The Retinoids: Biology, Chemistry and Medicine, second ed., Raven Press, New York, 1994.

[5] K. Niederreither, P. Dollé, Retinoic acid in development: towards an integrated view, Nat. Rev. Genet. 9 (2008) 541–553.

[6] D.J. Mangelsdorf, C. Thummel, M. Beato, P. Herrlich, G. Schiitq, K. Umesono, B. Blumberg, P. Kastner, M. Mark, P. Chambon, R.M. Evans, The nuclear receptor superfamily: the second decade, Cell 83 (1995) 835–839.

[7] R.A.S. Chandraratna, S.J. Gillett, T.K. Song, J. Attard, S. Vuligonda, M.E. Garst, T. Arefieg, D.W. Gil, L. Wheeler, Synthesis and pharmacological activity of conformationally restricted, acetylenic retinoid analogs, Bioorg. Med. Chem. Lett. 5 (1995) 523–527.

[8] M.A. Smith, D.R. Parkinson, B.D. Cheson, M.A. Friedman, Retinoids in cancer therapy, J. Clin. Oncol. 10 (1992) 839–864.

[9] J.C. Rhee, F.R. Khuri, D.M. Shin, Advances in chemoprevention of head and neck cancer, The Oncologist 9 (2004) 302–311.

[10] T.R.J. Evans, S.B. Kaye, Retinoids: present role and future potential, Br. J. Cancer 80 (1999) 1–8.

[11] D.R. Soprano, P. Qin, K.J. Soprano, Retinoic acid receptors and cancers, Annu. Rev. Nutr. 24 (2004) 201–221.

[12] N. Clarke, P. Germain, L. Altucci, H. Gronemeyer, Retinoids: potential in cancer prevention and therapy, Expert Rev. Mol. Med. 6 (2004) 1–23.

[13] C.S. Mizuno, S. Paul, N. Suh, A.M. Rimando, Synthesis and biological evaluation of retinoid-chalcones as inhibitors of colon cancer cell growth, Bioorg. Med. Chem. Lett. 20 (2010) 7385–7387.

[14] M.D. Collins, G.E. Mao, Teratology of retinoids, Annu. Rev. Pharmacol. Toxicol. 39 (1999) 399–430.

[15] R. Sharma, R. Sharma, U. Verma, N.K. Bhat, Drug review: novel drugs targeting retinoic acid receptors, JK Sci. J. Med. Educ. Res. 7 (2005).

[16] M. David, E. Hodak, N.J. Lowe, Adverse effects of retinoids, Med. Toxicol. Advers. Drug Exp. 3 (1988) 273–288.

[17] A.K. Silverman, C.N. Ellis, J.J. Voorhees, Hypervitaminosis A syndrome: a paradigm of retinoid side effects, J. Am. Acad. Dermatol. 16 (1987) 1027–1039.

[18] M.F. Boehm, L. Zhang, B.A. Badea, S.K. White, D.E. Mais, E. Berger, C.M. Suto, M.E. Goldman, R.A. Heyman, Synthesis and structure-activity relationships of novel retinoid X receptor-selective retinoids, J. Med. Chem. 37 (1994) 2930–2941.

[19] S. Biswal, U. Sahoo, S. Sethy, H.K.S. Kumar, M. Banerjee, Indole: the molecule of diverse biological activities, Asian J. Pharm. Clin. Res. 5 (2012) 1–6.

[20] P. Revill, N. Mealy, N. Serradell, J. Bolos, E. Rosa, Panobinostat, Drugs of the Future 32 (2007) 315.

[21] H.M. Prince, M. Bishton, Panobinostat (LBH589): A Novel Pan-deacetylase Inhibitor with Activity in T Cell Lymphoma, Hematology Meeting Reports, vol. 3, Peter MacCallum Cancer Centre and University of Melbourne, Parkville, Australia, 2009, pp. 33–38.

[22] P. Nikolinakos, J.V. Heymach, The tyrosine kinase inhibitor cediranib for non-small cell lung cancer and other thoracic malignancies, J. Thorac. Oncol. 3 (2008) S131–S134.

[23] B.B. Aggarwal, H. Ichikawa, Molecular targets and anticancer potential of indole-3-carbinol and its derivatives, Cell Cycle 4 (2005) 1201–1215.

[24] A.L. Fields, D.R. Soprano, K.J. Soprano, Retinoids in biological control and cancer, J. Cell. Biochem. 102 (2007) 886–898.

[25] Z. Ates-Alagoz, T. Coban, E. Buyukbingol, Synthesis and antioxidant activity of new tetrahydro-naphthalene-indole derivatives as retinoid and melatonin analogs, Arch. Pharm. Chem. Life Sci. 339 (2006) 193–200.

[26] T.F. Wood, W.M. Easter Jr., M.S. Carpenter, J. Angiolini, Polycyclic musks. I. Acyl-and dinitropolyalkyltetralin derivatives, J. Org. Chem. 28 (1963) 2248–2255.

[27] M.D. Collins, R.W. Curley Jr., M. Clagett-Dame, V.V. Abzianidze, A-[(*E*)-2-(5,6,7,8-tetrahydro-5,5,8,8-tetramethyl-2-napthalenyl)-1-propenyl]benzoic acid analogs and method of manufacture and use thereof, WO 2007005568 (2007).

[28] D.R. Adams, J.M. Bentley, J.R.A. Roffey, R.J. Hamlyn, S. Gaur, M.A.J. Duncton, J.E.P. Davidson, M.J. Bickerdike, I.A. Cliffe, H.L. Mansell, Pyrroloindoles, pyridoindoles and azepinoindoles as 5-ht2c agonists, US 6433175 (2002).

[29] A.S. Gurkan, A. Karabay, Z. Buyukbingol, A. Adejare, E. Buyukbingol, Syntheses of novel indole lipoic acid derivatives and their antioxidant effects on lipid peroxidation, Arch. Pharm. Chem. Life Sci. 338 (2005) 67–73.

[30] Z. Ates-Alagoz, Z. Buyukbingol, E. Buyukbingol, Synthesis and antioxidant properties of some indole ethylamine derivatives as melatonin analaogs, Pharmazie 60 (2005) 643–647.

[31] Y.-H. Ge, Y.-M. Wu, Z.-J. Xue, Synthesis of substituted indole-3-carboxaldehyde derivatives, Youji Huaxue 26 (2006) 563–567.

[32] F.A. Davis, B.-C. Chen, Enantioselective synthesis of (+)-O-trimethylsappanone B and (+)-O-trimethylbrazilin, J. Org. Chem. 58 (1993) 1751–1753.

[33] E. Dolusic, P. Larrieu, L. Moineaux, V. Stroobant, L. Pilotte, D. Colau, L. Pochet, B.V. den Eynde, B. Masereel, J. Wouters, R. Frederick, Tryptophan 2,3-dioxygenase (TDO) inhibitors. 3-(2-(pyridyl)ethenyl)indoles as potential anticancer immunomodulators, J. Med. Chem. 54 (2011) 5320–5334.

[34] R.H. Shoemaker, The NCI60 human tumour cell line anticancer drug screen, Nat. Rev. Cancer 6 (2006) 813–823.

[35] I.P. Uray, P.H. Brown, Chemoprevention of hormone receptor-negative breast cancer: new approaches needed, Recent Results Cancer Res. 188 (2011) 147–162.

[36] C.M. Perou, T. Sorlie, M.B. Eisen, M. van de Rijn, S.S. Jeffrey, C.A. Rees, J.R. Pollack, D.T. Ross, H. Johnsen, L.A. Akslen, O. Fluge, A. Pergamenschikov, C. Williams, S.X. Zhu, P.E. Lønning, A.L. Børresen-Dale, P.O. Brown, D. Botstein, Molecular portraits of human breast tumors, Nature 406 (2000) 747–752.

[37] T. Sorlie, R. Tibshirani, J. Parker, T. Hastie, J.S. Marron, A. Nobel, S. Deng, H. Johnsen, R. Pesich, S. Geisler, J. Demeter, C.M. Perou, P.E. Lønning, P.O. Brown, A.L. Børresen-Dale, D. Botstein, Repeated observation of breast tumor subtypes in independent gene expression data sets, Proc. Natl. Acad. Sci. U. S. A. 100 (2003) 8418–8423.

[38] E. Charafe-Jauffret, C. Ginestier, F. Monville, P. Finetti, J. Adelaide, N. Cervera, S. Fekairi, L. Xerri, J. Jacquemier, D. Birnbaum, F. Bertucci, Gene expression profiling of breast cell lines identifies potential new basal markers, Oncogene 25 (2006) 2273–2284.

[39] A.A. Onitilo, J.M. Engel, R.T. Greenlee, B.N. Mukesh, Breast cancer subtypes based on ER/PR and Her2 expression: comparison of clinicopathologic features and survival, Clin. Med. Res. 7 (2009) 4–13.

[40] X.H. Tang, L.J. Gudas, Retinoids, retinoic acid receptors, and cancer, Annu. Rev. Pathol. Mech. Dis. 6 (2011) 345–364.

[41] A.N. Fanjul, D. Delia, M.A. Pierotti, D. Rideout, J. Qiu, M. Pfahl, 4-Hydroxyphenyl retinamide is a highly selective activator of retinoid receptors, J. Biol. Chem. 271 (1996) 22441–22446.

[42] M.A.C. Pratt, M. Niu, D. White, Differential regulation of protein expression, growth and apoptosis by natural and synthetic retinoids, J. Cell. Biochem. 90 (2003) 692–708.

[43] W.P. Lippert, C. Burschka, K. Gotz, M. Kaupp, D. Ivanova, C. Gaudon, Y. Sato, P. Antony, N. Rochel, D. Moras, H. Gronemeyer, R. Tacke, Crystal structure of the human RXR alpha ligand binding domain bound to a synthetic agonist compound and a coactivator peptide, ChemMedChem 4 (2009) 1143–1152.

[44] B.P. Klaholz, J.P. Renaud, A. Mitschler, C. Zusi, P. Chambon, H. Gronemeyer, D. Moras, Conformational adaptation of agonists to the human nuclear receptor RAR gamma, Nat. Struct. Biol. 5 (1998) 199–202.

[45] J.P. Renaud, N. Rochel, M. Ruff, V. Vivat, P. Chambon, H. Gronemeyer, D. Moras, Crystal structure of the RAR-gamma ligand-binding domain bound to all-trans retinoic acid, Nature 378 (1995) 681–689.

[46] G.M. Morris, D.S. Goodsell, R.S. Halliday, R. Huey, W.E. Hart, R.K. Belew, A.J. Olson, Automated docking using a Lamarckian genetic algorithm and empirical binding free energy function, J. Comput. Chem. 19 (1998) 1639–1662.

[47] D.A. Case, T.A. Darden, T.E. Cheatham III, C.L. Simmerling, J. Wang, R.E. Duke, R. Luo, R.C. Walker, W. Zhang, K.M. Merz, B.P. Roberts, B. Wang, S. Hayik, A. Roitberg, G. Seabra, I. Kolossvai, K.F. Wong, F. Paesani, J. Vanicek, J. Liu, X. Wu, S.R. Brozell, T. Steinbrecher, H. Gohlke, Q. Cai, X. Ye, J. Wang, M.-J. Hsieh, G. Cui, D.R. Roe, D.H. Mathews, M.G. Seetin, C. Sagui, V. Babin, T. Luchko, S. Gusarov, A. Kovalenko, P.A. Kollman, AMBER 11, University of California, San Francisco, 2010.

[48] K. Lindorff-Larsen, S. Piana, K. Palmo, P. Maragakis, J.L. Klepeis, R.O. Dror, D.E. Shaw, Improved side-chain torsion potentials for the Amber ff99SB protein force field, Proteins 78 (2010) 1950–1958.

[49] V. Hornak, R. Abel, A. Okur, B. Strockbine, A. Roitberg, C. Simmerling, Comparison of multiple Amber force fields and development of improved protein backbone parameters, Proteins 65 (2006) 712–725.

[50] D.A. Case, T.E. Cheatham III, T. Darden, H. Gohlke, R. Luo, K.M. Merz Jr., A. Onufriev, C. Simmerling, B. Wang, R. Woods, The Amber biomolecular simulation programs, J. Comput. Chem. 26 (2005) 1668–1688.

[51] A. Onufriev, D. Bashford, D.A. Case, Exploring protein native states and large-scale conformational changes with a modified generalized Born model, Proteins 55 (2004) 383–394.

[52] R.W. Pastor, B.R. Brooks, A. Szabo, An analysis of the accuracy of Langevin and molecular dynamics algorithms, Mol. Phys. 65 (1988) 1409–1419.

[53] J. Antony, D.M. Medvedev, A.A. Stuchebrukhov, Theoretical study of electron transfer between the photolyase catalytic cofactor FADH(−) and DNA thymine dimer, J. Am. Chem. Soc. 122 (2000) 1057–1065.

[54] W.D. Cornell, P. Cieplak, C.I. Bayly, I.R. Gould, K.M. Merz Jr., D.M. Ferguson, D.C. Spellmeyer, T. Fox, J.W. Caldwell, P.A. Kollman, A second generation force field for the simulation of proteins, nucleic acids, and organic molecules, J. Am. Chem. Soc. 117 (1995) 5179–5197.

[55] D. Sitkoff, K.A. Sharp, B. Honig, Accurate calculation of hydration free energies using macroscopic solvent models, J. Phys. Chem. 98 (1994) 1978–1988.

[56] J. Srinivasan, T.E. Cheatham III, P. Cieplak, P.A. Kollman, D.A. Case, Continuum solvent studies of the stability of DNA, RNA, and phosphoramidate-DNA helices, J. Am. Chem. Soc. 120 (1998) 9401–9409.

[57] D.A. Case, Molecular dynamics and normal mode analysis of biomolecular rigidity, in: M.F. Thorpe, P.M. Duxbury (Eds.), Rigidity Theory and Applications, Plenum, 1999, pp. 329–344.

[58] H. Gohlke, D.A. Case, Converging free energy estimates: MM-PB(GB)SA studies on the protein–protein complex Ras-Raf, J. Comput. Chem. 25 (2004) 238–250.